Korean J. Chem. Eng., 35(12), 2480-2486 (2018)
DOI: 10.1007/s11814-018-0176-8

pISSN: 0256-1115
eISSN: 1975-7220

Spray pyrolysis synthesis of mesoporous TiO_2 microspheres and their post modification for improved photocatalytic activity

Jaehyung Choi*, Kye Sang Yoo,†, and Jinsoo Kim*,†**

*Department of Chemical Engineering, Kyung Hee University, 1732 Deogyeong-daero, Giheung-gu, Yongin-si, Gyeonggi-do 17104, Korea
**Department of Chemical & Biomolecular Engineering, Seoul National University of Science and Technology, 232 Gongneung-ro, Nowon-gu, Seoul 01811, Korea
(*Received 5 September 2018 • accepted 16 October 2018*)

Abstract−Mesoporous TiO_2 microspheres were prepared by spray pyrolysis for photocatalysis. Post modification of TiO_2 by heat treatment was performed to optimize its photocatalytic performance. First, spherical TiO_2 particles with mesoporous structure were synthesized at pyrolysis temperatures of 500, 600, and 700 °C. After characterization by XRD, SEM, and N_2 adsorption, a sample prepared at 500 °C was found to possess desirable properties for photocatalytic performance through post-modification. In methylene blue degradation, mesoporous TiO_2 microspheres synthesized at 500 °C outperformed other microspheres. Furthermore, samples obtained by spray pyrolysis at 500 °C were calcined at various temperatures as a post-modification process. The sample calcined at 350 °C showed improved photocatalytic activity due to optimal anatase crystallinity and surface area.

Keywords: Post Modification, Mesoporous TiO_2 Spheres, Spray Pyrolysis, MB Degradation

INTRODUCTION

With the pioneering discovery of the photocatalytic properties of TiO_2 and its environmentally benign properties (i.e., non-toxic, lack of dissolution in water, and light stability), TiO_2 photocatalysts are important not only for killing pathogenic microorganisms but also to decompose persistent organic contaminants in water [1,2]. TiO_2 produces hydroxyl radicals that are extremely reactive and readily attack organic pollutants when irradiated by UV light. As a result, organic pollutants are sequentially converted to simpler organic molecules that eventually are mineralized to CO_2, H_2O, and mineral species [3-5]. Generally, the TiO_2 photocatalytic decomposition reaction is characterized by a high reaction rate and short processing time due to rapid hydroxyl radical-based oxidation reactions. However, TiO_2 photocatalytic activity has a major disadvantage of low light utilization efficiency, which is due to relatively large particle size and low surface area, a need for UV, low catalyst porosity, and crystal structure. Thus, it is necessary to improve catalytic activity to overcome the barrier of a commercialization process as a full-scale technology.

Together with surface area, the crystal structure and crystallinity of titania particles are important factors that determine photocatalytic activity [6-9]. Anatase TiO_2 is generally accepted as being the most reactive crystalline phase among amorphous, anatase, brookite, and rutile phases [10]. Generally, a sol-gel process carried out in an excess of a water-containing solvent mixture results in amorphous TiO_2 particles with no photocatalytic activity. Heat treatment is necessary for crystallization even though it causes a drastic decrease in the TiO_2 surface area due to pore shrinkage and disintegration [11-13]. Therefore, it is crucial to synthesize highly porous anatase TiO_2 particles with high surface area and narrow pore size distribution, for higher accessibility of reactants at the active site, to develop a practical photocatalytic process.

As an extension of the preparation of metal oxides with mesoporosity, mesoporous TiO_2 is usually synthesized using the sol-gel method with a self-assembly template. This technique consists of several steps including hydrolysis and condensation, filtration, washing, and calcination to remove surfactant [14-21]. On the other hand, the instability of mesostructures after calcination [22,23], the expense of additives, and the complication of the multi-step process limit practical application of current synthesis methods. Spray pyrolysis, widely used for industrial powder production, has desirable flexibility and industrial feasibility in the preparation of conventional TiO_2 materials [24-26]. In this method, after the sprayed liquid of the precursor solution undergoes evaporation and shrinkage, it flows through the high-temperature reactor to finally form solid particles. Using this technique, spherical TiO_2 particles can be produced without an additional pelletization step.

We synthesized titanium dioxide microspheres with mesoporous structure by spray pyrolysis without templating reagents as a photocatalysis for methylene blue degradation. Methylene blue (MB) degradation has been recommended in standard procedures for evaluating the photocatalytic activity in wastewater treatment. The influence of important synthesis parameters including pyrolysis temperature and post-calcination temperature on the structural and photocatalytic properties of TiO_2 spheres was systematically investigated. Compared with a conventional batch-type sol-gel process, spray pyrolysis is a continuous process that is amenable to mass produc-

†To whom correspondence should be addressed.
E-mail: kyoo@snut.ac.kr, jkim21@khu.ac.kr

tion of controllable materials. Notably, TiO_2 of high purity and spherical shape could be synthesized in one step as a photocatalyst for removal of organic pollutants.

EXPERIMENTAL

1. TiO_2 Sol Preparation

0.5 M of TiO_2 sol precursor was prepared using hydrolysis and condensation of TTIP (titanium (IV) isopropoxide, 97% Aldrich) in isopropyl alcohol (99.7%, Carlo) medium with DI water. In brief, 0.25 mol of TTIP was mixed with 100 ml of isopropyl alcohol. The solution was stirred vigorously using a magnetic stirrer for 30 min. For hydrolysis of TTIP, 300 ml of DI water was added dropwise into the previously mixed solution. After complete addition of DI water, the resulting solution was stirred for four hours in an oil bath maintained at 95 °C. Next, 70 ml of 1 M nitric acid was added for peptization, and the solution was stirred and refluxed in an oil bath at 95 °C for 24 hours. After reflux, DI water was added to make a 0.5 M TiO_2 sol, followed by aging for two days at room temperature.

2. Spray Pyrolysis

The spray pyrolysis system was composed of spray zone, heating zone, and powder collecting zone as reported in previous literature [27,28]. TiO_2 sol was nebulized with six ultrasonic vibrators (1.7 MHz) and carried to the heating zone by nitrogen gas. The temperature of the heating zone was controlled with a PID controller with two furnaces. Synthesized TiO_2 particles were collected by thimble filter in the collection zone. The collection zone was heated to 170 °C with heating tape to maintain drying conditions.

3. Characterizations

The pore structure and BET surface area of the samples were analyzed using N_2 porosimetry (Tristar 3020, Micromeritics, USA). All samples were degassed under vacuum at 150 °C for six hours before measurement. The phase structure and crystallinity of the samples were investigated by X-ray diffraction (XRD; Miniflex 600, Rigaku, Japan), with a Cu Kα radiation source (λ=1.54 Å) and a 2θ range from 20° to 90° at a scanning rate of 6°/min. The morphology of the synthesized particles was analyzed using a high-resolution field emission scanning electron microscope (HR FE-SEM; MERLIN, Carl Zeiss, Germany).

4. Photocatalytic Activity Test

The photocatalytic activity of TiO_2 powder was investigated by monitoring degradation of methylene blue (MB) dye in aqueous solution under ultra-violet (UV) light. 100 ml of suspension containing MB solution and TiO_2 powder was prepared by completely dissolving MB dye in DI water to give a concentration of 20 ppm, and 0.1 g of pre-synthesized TiO_2 powder was dispersed in the MB aqueous solution. The suspension was stirred in the dark for one hour to stabilize the adsorption of MB dye over the surface of TiO_2 powder. The stable suspension was irradiated with UV-light emitted from a 400 W mercury lamp with wavelengths in the range of 200-400 nm under continuous stirring. The reactor was maintained at 25 °C using a circulating water bath. During the photodegradation process, the concentration of MB solution was analyzed at determined times by UV-visible spectrophotometry (Optizen POP, Mecasys, Korea).

RESULTS AND DISCUSSION

1. Effect of Pyrolysis Temperature

The spray pyrolysis technique was utilized to synthesize spherical mesoporous TiO_2 catalysts with optimal photocatalytic efficiency. A typical spray pyrolysis process always includes four major steps: formation of droplets from a precursor solution, reduction of droplet size by evaporation, conversion of precursor to oxide, and for-

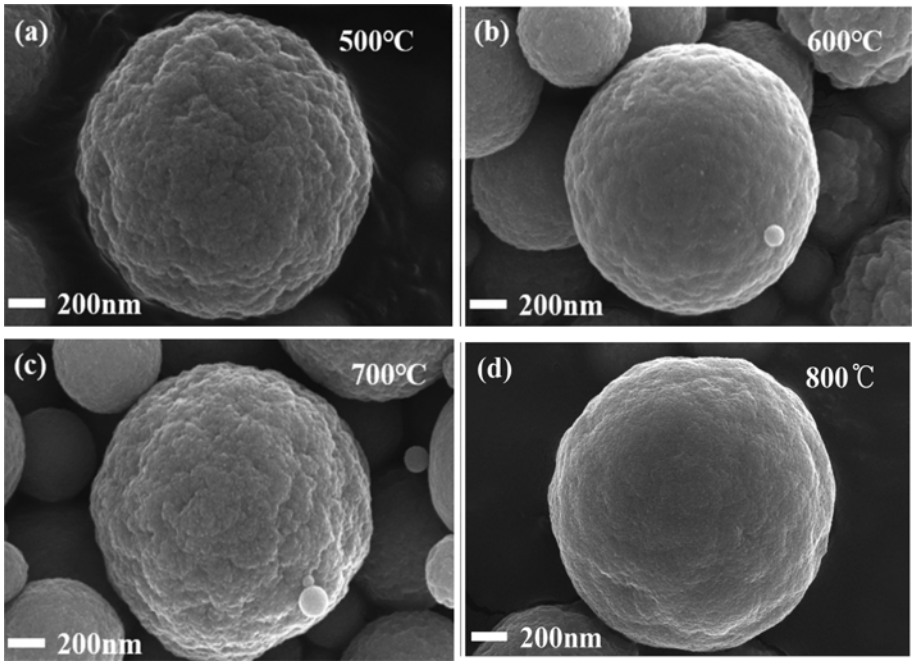

Fig. 1. HR FE-SEM images of TiO_2 microspheres prepared at various pyrolysis temperatures (a) 500 °C, (b) 600 °C, (c) 700 °C and (d) 800 °C.

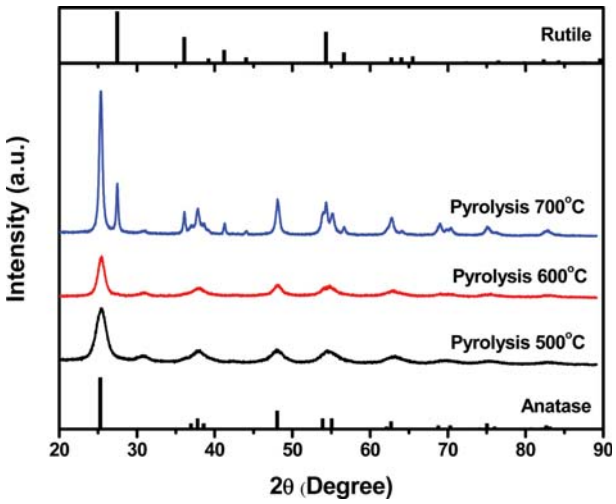

Fig. 2. XRD patterns of TiO_2 prepared by spray pyrolysis at various pyrolysis temperatures.

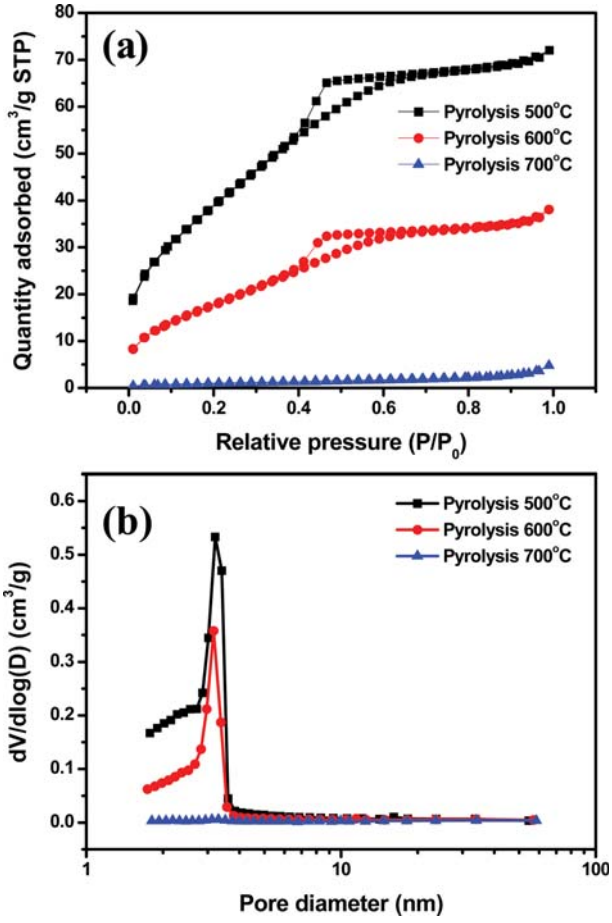

Fig. 3. (a) Adsorption and desorption isotherms and (b) pore size distributions of TiO_2 microspheres prepared by spray pyrolysis at various pyrolysis temperatures.

mation of solid particles. Solvent evaporation, solute diffusion, drying and pyrolysis can occur during particle formation, in which evaporation of solvent has been demonstrated to be important for particle porosity. Water evaporates from droplets of atomized TiO_2 sol to form a viscous saturated droplet. Colloidal particles contained in this droplet are inter-connected to form a porous structure. Water in the formed inner-space evaporates to provide pores in the sphere. After excess water removal, an oxide completely forms. Thus, pyrolysis temperature plays a crucial role in the evaporation rate of water in this process.

Initially, TiO_2 particles were synthesized at various pyrolysis temperatures of 500, 600, 700 and 800 °C under identical experiment conditions. The morphology of TiO_2 particles was analyzed by SEM characterization. As shown in Fig. 1, uniform spherical TiO_2 particles of 1.5 micrometers formed regardless of the spray pyrolysis temperature. Interestingly, the shape of TiO_2 particles prepared at 800 °C was hardly affected as shown in Fig. 1(d), even though the crystal structure of the sample was already transformed to rutile phase (not shown). Thus, a uniform spherical particle might be maintained under the entire synthesis conditions in this study. This result is very desirable because the particle shape prepared by this technique could be used directly in commercial processes without further modification. XRD characterization was used to determine the crystal structure of TiO_2 spheres. The crystallinity of the particles with spray pyrolysis temperature is shown in Fig. 2. It was observed that the crystallinity of TiO_2 spheres increased with increasing pyrolysis temperature. The TiO_2 sample prepared at 600 °C showed the highest anatase crystallinity, and the crystalline phase began to transform into rutile phase at 700 °C.

Structural properties of the samples were measured by the nitrogen adsorption method. Adsorption-desorption curves of TiO_2 spheres prepared by spray pyrolysis at various pyrolysis temperatures are shown in Fig. 3(a). Typical type IV (IUPAC classification) curves were observed for samples prepared at 500 and 600 °C [29, 30]. Typical features of the Type IV isotherm are its hysteresis loop, which is associated with capillary condensation taking place in mesopores, and the limiting uptake over a range of high P/P_0. However, the mesoporous structure of TiO_2 spheres was completely decom-

Table 1. Structural properties of TiO_2 synthesized by spray pyrolysis at various pyrolysis temperatures without and with calcination at 450 °C for 3 h

Pyrolysis temperature		500 °C	600 °C	700 °C
BET surface area (m^2/g)	Before calcination	149.4	68.7	3.58
	After calcination	73.4	11.3	3.61
Total pore volume (cm^3/g)	Before calcination	0.094	0.052	0.0067
	After calcination	0.096	0.014	0.0076

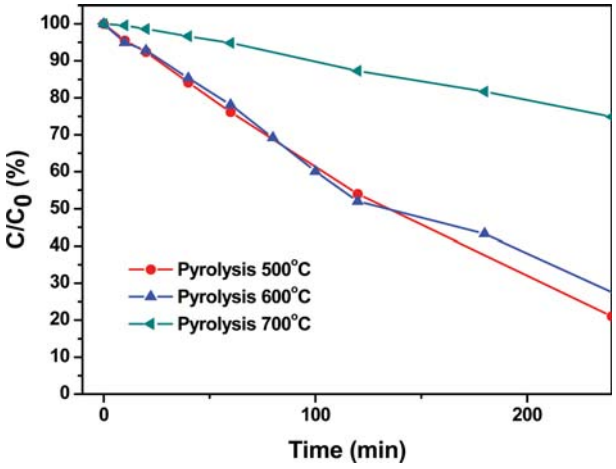

Fig. 4. Photocatalytic activity of TiO_2 microspheres prepared by spray pyrolysis at various pyrolysis temperatures for MB degradation.

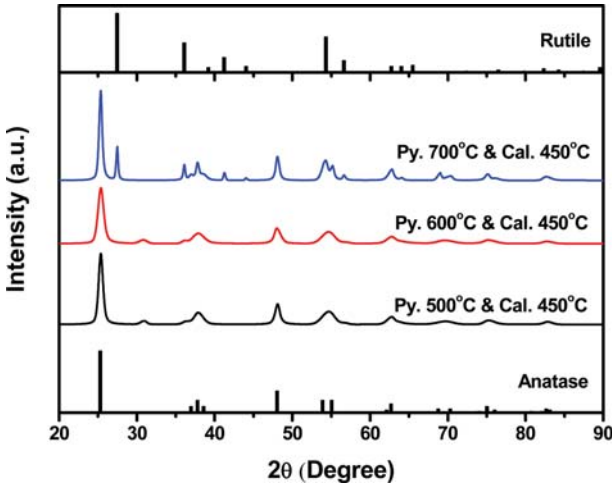

Fig. 5. XRD patterns of TiO_2 prepared by spray pyrolysis at various pyrolysis temperatures followed by calcination at 450 °C for 3 h.

posed for the sample prepared at a higher pyrolysis temperature (700 °C). Pore size distributions of the prepared samples are shown in Fig. 3(b). For samples prepared at 500 and 600 °C, pores of about 3 nm were similarly formed. However, no mesopores were formed in the sample prepared at 700 °C.

The specific surface area and pore volume of samples prepared at various pyrolysis temperatures are illustrated in Table 1. The specific surface area of the synthesized spheres decreased sharply with an increase in pyrolysis temperature, which is due to sintering between the particles at higher pyrolysis temperature. In particular, in the temperature range where the phase transition occurs, the specific surface area decreased rapidly from the decrease in space between crystals. Similar trends were observed for the pore volumes of the samples (see Table 1).

The decomposition of MB was measured to evaluate the photocatalytic activity of TiO_2 spheres synthesized at various pyrolysis temperatures, as shown in Fig. 4. Microspheres synthesized at 500 and 600 °C showed similar photocatalytic efficiency. However, the TiO_2 sample synthesized at 700 °C showed a relatively low decomposition rate. This result is mainly attributed to phase transition to the rutile phase and the very low specific surface area of the sample. This result can be explained by semiconductor theory. After illumination of the photocatalyst by photons with adequate energy, an electron in the valence band becomes excited and jumps to the conduction band, leaving a positively charged hole in the valence band. The photocatalyst generates electron-hole (e^-/h^+) pairs at the surface. Besides recombination with the electron, the positively charged hole on the surface of TiO_2 can oxidize adsorbed water to produce hydroxyl radicals ($OH^•$). Meanwhile, the excited electron can react with a dissolved oxygen molecule to form superoxide anion radical ($O_2^{•-}$) and H_2O_2, subsequently producing hydroxyl radicals. Reactive species, such as h^+, $OH^•$, and $O_2^{•-}$ play an important role in the decolorization of MB. These species have strong oxidation ability and react readily with surface adsorbed organic pollutants [31,32].

2. Effect of Post-modification

As mentioned, the change in surface properties of TiO_2 by heat treatment has a great influence on photocatalytic efficiency. For this reason, post-modification was performed to improve photocatalytic performance of the prepared TiO_2 spheres. TiO_2 spheres synthesized by thermal spraying at various temperatures were calcined at 450 °C for three hours to evaluate the effect of post-modification. First, crystal structures of the samples were determined by XRD analysis. Slight changes in the crystal structures were observed after calcination of samples prepared at 500 and 600 °C. Indeed, the crystallinity of the anatase crystal phase increased slightly, as shown in Fig. 5. However, the sample synthesized at 700 °C appeared to have little change from post-modification. Comparable results were observed for the structural properties of the samples. The specific surface area of the samples synthesized at 500 °C and 600 °C significantly changed, as illustrated in Table 1; however, no noticeable change was observed for the sample synthesized at 700 °C.

The analysis of nitrogen isotherms showed a comparable tendency, as shown in Fig. 6(a). A typical mesoporous structure was more clearly formed for the sample prepared at 500 °C. However, meso-porosity of the sample synthesized at 600 °C was found to be significantly collapsed. No significant change was observed for the sample synthesized at 700 °C even after post-modification. The effect of post-modification on the pore size distribution is shown in Fig. 6(b). Post-modification slightly affected the pore size distribution, and the pore size slightly increased to 3.5 nm after calcination.

MB removal experiments using mesoporous TiO_2 spheres were performed to investigate the effect of post-modification, as shown in Fig. 7. Interestingly, the post-modification effect for the sample prepared at 500 °C was very significant, which is mainly attributed to an increase in the crystallinity of the anatase phase, the main factor for photocatalytic efficiency. For the sample synthesized at 600 °C, photocatalytic efficiency slightly increased, because although anatase phase crystallinity increased, the specific surface area of the catalyst decreased considerably. The sample synthesized at 700 °C did not show any modification effect on photocatalytic activity. Therefore, it is most preferable to synthesize mesoporous TiO_2 spheres at 500 °C to maximize the post-modification effect.

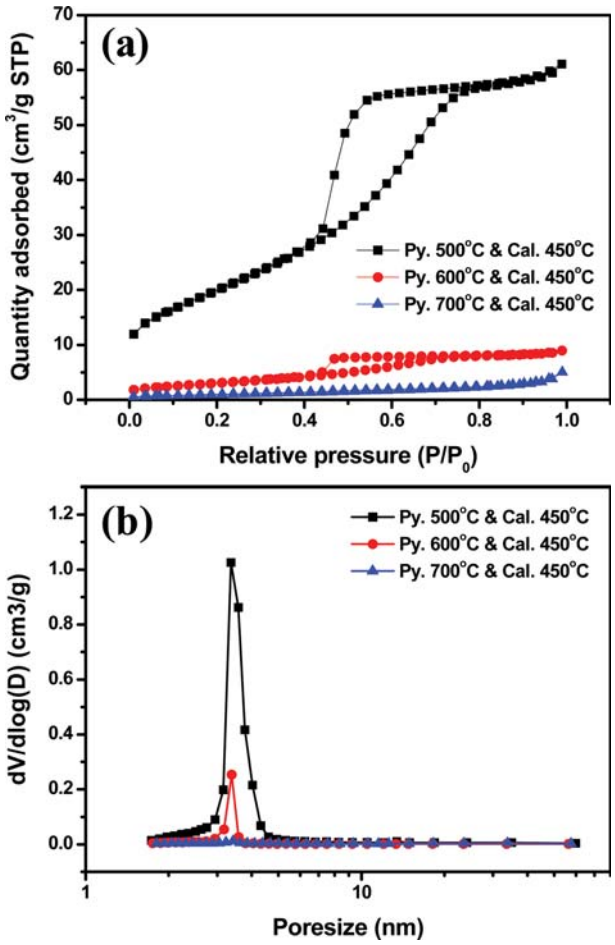

Fig. 6. (a) Adsorption and desorption isotherms and (b) pore size distributions of TiO_2 microspheres prepared by spray pyrolysis at various pyrolysis temperatures followed by calcination at 450 °C for 3 h.

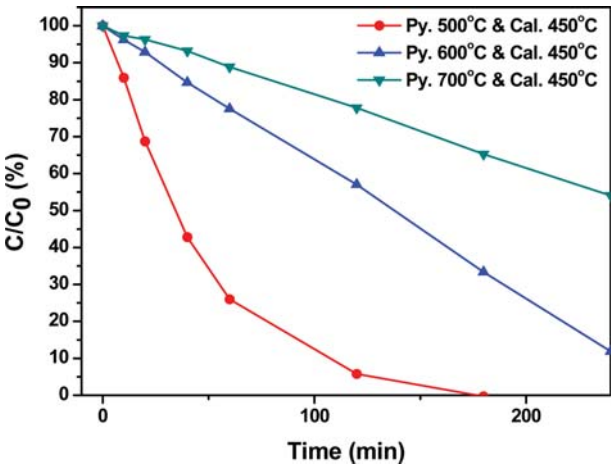

Fig. 7. Photocatalytic activity of TiO_2 microspheres prepared by spray pyrolysis at various pyrolysis temperatures followed by calcination at 450 °C for 3 h in MB degradation.

For optimization of the post-modification process, the TiO_2 sample prepared at 500 °C was calcined at various temperatures for three hours. The samples were heat treated at 250, 350, and 450 °C. As shown in Fig. 8, the crystallinity of the anatase structure improved with higher calcination temperature. In particular, the sample calcined at 450 °C had the highest crystallinity. Nitrogen porosimetry was used to analyze the structural characteristics of the samples. As illustrated in Table 2, specific surface area and pore volume of the samples slightly changed up to the calcination temperature of 350 °C. After calcination at 450 °C, however, the specific surface area decreased and pore size increased. Structural characteristics of the samples were analyzed by adsorption/desorption curves as shown in Fig. 9(a). No significant change was observed until the calcination temperature reached 350 °C. However, for the sample calcined at 450 °C, mesoporous characteristics were apparent. For pore size distribution, there was little difference at these calcination temperatures. The effect of calcination temperature on photocatalytic activity is shown in Fig. 10. The mesoporous TiO_2 spheres calcined at 350 °C showed the highest photocatalytic activity among the samples, presumably due to the optimization of crystallinity of anatase crystals and specific surface area, which determine the efficiency of the photocatalyst.

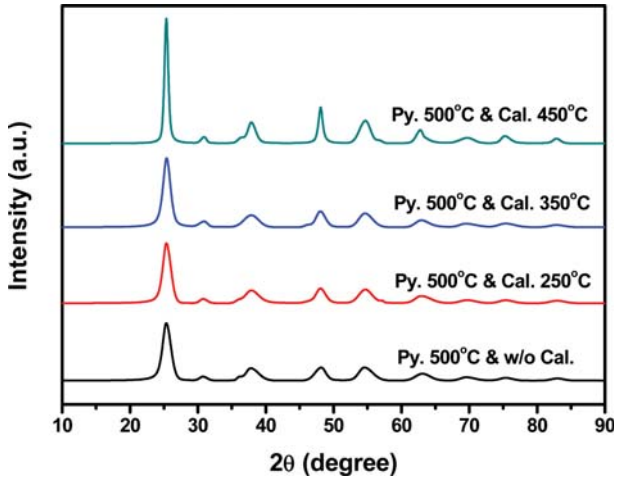

Fig. 8. XRD patterns of TiO_2 microspheres prepared by spray pyrolysis at 500 °C followed by calcination at various temperatures for 3 h.

Table 2. Structural properties of TiO_2 synthesized by spray pyrolysis at 500 °C followed by calcination at various temperatures for 3 h

Calcination temperature	-	250 °C	350 °C	450 °C
BET surface area (m^2/g)	149.4	144.0	139.3	73.4
Total pore volume (cm^3/g)	0.094	0.090	0.11	0.096

CONCLUSIONS

Mesoporous TiO_2 microspheres were synthesized continuously by means of a one-step spray pyrolysis process. Among the preparation conditions, pyrolysis temperature was a crucial parameter in determining the structural properties of TiO_2 materials. In the mechanism of sphere formation during spray pyrolysis, most of the steps

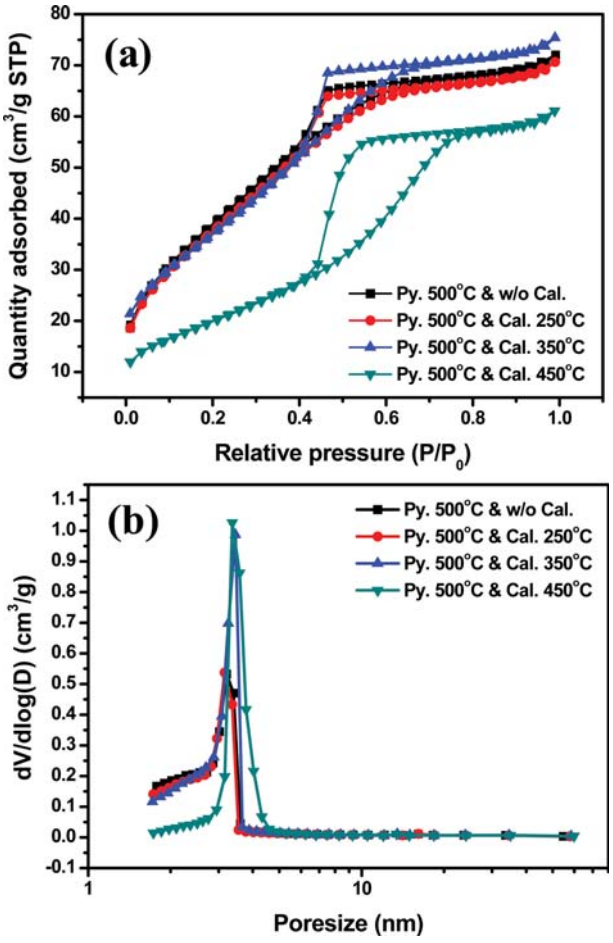

Fig. 9. (a) Adsorption and desorption isotherms and (b) pore size distributions of TiO_2 microspheres by spray pyrolysis at 500 °C followed by calcination at various temperatures for 3 h.

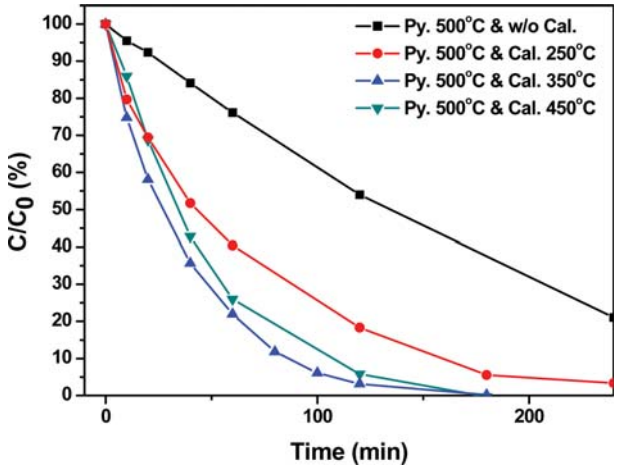

Fig. 10. Photocatalytic activity of TiO_2 microspheres prepared by spray pyrolysis at 500 °C followed by calcination at various temperatures for 3 h in MB degradation.

could be affected by pyrolysis temperature to form mesoporous spherical particles. The post-modification calcination process strongly affected the photocatalytic activity of TiO_2 microspheres. In MB degradation experiments, the sample prepared at 500 °C exhibited remarkable photocatalytic performance after calcination at 350 °C. Therefore, the spray pyrolysis method combined with post-modification process has potential for the synthesis of commercial photocatalysts.

ACKNOWLEDGEMENTS

This work was supported by the Basic Science Research Program through the National Research Foundation of Korea (NRF) funded by the Ministry of Education, Science and Technology (Grant NRF-2016R1A2B4014805) and the Engineering Research Center of Excellence Program of the Korea Ministry of Science, ICT & Future Planning (MSIP)/National Research Foundation of Korea (NRF) (Grant NRF-2014R1A5A1009799).

REFERENCES

1. H. M. Yadav, J. S. Kim and S. H. Pawar, *Korean J. Chem. Eng.*, **33**(7), 1989 (2016).
2. C. Lalhriatpuia, A. Tiwari, A. Shukla, D. Tiwari and S. M. Lee, *Korean J. Chem. Eng.*, **33**(12), 3367 (2016).
3. A. L. Linsebigler, G. Lu and J. T. Yates, *Chem. Rev.*, **95**, 735 (1995).
4. L. A. Lawton, P. K. J. Robertson, B. J. P. A. Cornish and M. Jaspars, *Environ. Sci. Technol.*, **33**(5), 771 (1999).
5. M. R. Hoffmann, S. T. Martin, W. Choi and D. W. Bahnemann, *Chem. Rev.*, **95**, 69 (1995).
6. J. Noh, M. Yi, S. Hwang, K. M. Im, T. Yu and J. Kim, *J. Ind. Eng. Chem.*, **33**, 369 (2016).
7. M. S. Song, K. Vijayarangamuthu, E. J. Han, K. J. Jeon and J. W. Seo, *Korean J. Chem. Eng.*, **33**(8), 2392 (2016).
8. T. Zhang, J. Low, K. Koh, J. Yu and T. Asefa, *ACS Sustain. Chem. Eng.*, **6**(1), 531 (2018).
9. Z. Yang, Y. Shi and B. Wang, *Appl. Surf. Sci.*, **31**, 192 (2017).
10. J. Schneider, M. Matsuoka, M. Takeuchi, J. Zhang, Y. Horiuchi, M. Anpo and D. W. Bahnemann, *Chem. Rev.*, **114**(19), 9919 (2014).
11. C. C. Wang and J. Y. Ying, *Chem. Mater.*, **11**(11), 3113 (1999).
12. K. S. Yoo, T. G. Lee and J. Kim, *Micropor. Mesopor. Mater.*, **84**, 211 (2005).
13. J. Choi, J. Kim, K. S. Yoo and T. G. Lee, *Powder Technol.*, **181**(1), 83 (2008).
14. C. Márquez-Alvarez, N. Žilková, J. Pérez-Pariente and J. Čejka, *Catal. Rev.*, **50**, 222 (2008).
15. J. Čejka, *Appl. Catal. A*, **254**, 327 (2003).
16. F. Vaudry, S. Khodabandeh and M. E. Davis, *Chem. Mater.*, **8**, 1451 (1996).
17. Y. Kim, P. Kim, C. Kim and J. Yi, *J. Mater. Chem.*, **13**, 2353 (2003).
18. I. Balint and A. Miyazaki, *Micropor. Mesopor. Mater.*, **122**, 216 (2009).
19. D. Hidalgo, R. Messina, A. Sacco, D. Manfredi, S. Vankova, E. Garroe, G. Saracco and S. Hernandez, *Int. J. Hydrog. Energy*, **39**(36), 21512 (2014).
20. R. M. Camara, R. Portela, F. Gutierrez-Martin and B. Sanchez, *Chem. Eng. J.*, **283**, 535 (2016).
21. S. Casino, F. Di Lupo, C. Francia, A. Tuel, S. Bodoardo and C. Gerbaldi, *J. Alloy Compd.*, **594**, 114 (2014).
22. M. Yada, H. Hiyoshi, K. Ohe, M. Machida and T. Kijima, *Inorg.*

Chem., **36**, 5565 (1997).
23. M. Yada, H. Kitamura, M. Machida and T. Kijima, *Langmuir*, **13**, 5252 (1997).
24. R. Strobel, A. Alfons and S. E. Pratsinis, *Adv. Powder Technol*., **17**, 457 (2006).
25. O. Arutanti, A. B. D. Nandiyanto, T. Ogi, F. Iskandar, T. O. Kim and K. Okuyama, *J. Alloy Compd*., **591**, 121 (2014).
26. L. G. Bettini, M. V. Dozzi, F. D. Foglia, G. L. Chiarello, E. Selli, C. Lenardi, P. Piseri and P. Milani, *Appl. Catal. B: Environ*., **178**, 226 (2015).
27. H. Choi, D. Kim, S. P. Yoon, J. Han, S. Ha and J. Kim, *J. Anal. Appl. Pyrolysis*, **112**, 276 (2015).
28. H. Choi, S. P. Yoon, J. Han, J. Kim and M. R. Othman, *J. Ind. Eng. Chem*., **47**, 254 (2017).
29. K. S. W. Sing, *Carbon*, **32**, 1311 (1994).
30. M. D. Donohue and G. L. Aranovich, *Adv. Colloid Interface Sci*., **76-77**, 137 (1998).
31. J. Tang, J. R. Durrant and D. R. Klug, *J. Am. Chem. Soc*., **130**, 13885 (2008).
32. X. Li, C. Chen and J. Zhao, *Langmuir*, **17**, 4118 (2001).